Available online at www.sciencedirect.com
ScienceDirect
Engineering Fracture Mechanics 74 (2007) 1041–1053
Engineering Fracture Mechanics
www.elsevier.com/locate/engfracmech

Self-similarity and crack growth instability in the correlation between the Paris' constants

Alberto Carpinteri *, Marco Paggi

Politecnico di Torino, Department of Structural and Geotechnical Engineering, Corso Duca degli Abruzzi 24, 10129 Torino, Italy

Available online 31 January 2007

Abstract

In this note the question about the existence of a correlation between the parameters C and m of the Paris' law is re-examined. According to dimensional analysis and incomplete self-similarity concepts applied to the linear range of fatigue crack growth, a power-law asymptotic representation relating the parameter C to m and to the governing variables of fatigue is derived. Then, from the observation that the Griffith–Irwin instability must coincide with the Paris' instability at the onset of rapid crack growth, the exponents entering this correlation are determined. A fair good agreement is found between the proposed theory and extensive experimental data.

Keywords: Fatigue crack growth; Paris' law; Paris' constants; Dimensional analysis; Incomplete self-similarity; Crack growth instability; Loading ratio

1. Introduction

Fatigue crack growth data for ductile materials are usually presented in terms of the crack growth rate, $\mathrm{d}a/\mathrm{d}N$, and the stress–intensity factor range, $\Delta K = (K_{\max} - K_{\min})$. At present, it is a common practice to describe the process of fatigue crack growth by a logarithmic $\mathrm{d}a/\mathrm{d}N$ vs. ΔK diagram (see e.g. Fig. 1).

Three regions are generally recognized on this diagram for a wide collection of experimental results [1]. The first region corresponds to stress–intensity factor ranges near a lower threshold value, ΔK_{th}, below which no crack propagation takes place. This region of the diagram is usually referred to as *Region I*, or the near-threshold region [2]. The second linear portion of the diagram defines a power-law relationship between the crack growth rate and the stress–intensity factor range and is usually referred to as *Region II* [3]. Finally, when $K_{\max}$ tends to the critical stress–intensity factor, K_{IC}, rapid crack propagation takes place and crack growth instability occurs (*Region III*) [4].

* Corresponding author. Tel.: +39 011 564 4850; fax: +39 011 564 4899.
E-mail address: alberto.carpinteri@polito.it (A. Carpinteri).

0013-7944/$ - see front matter
doi:10.1016/j.engfracmech.2006.12.007

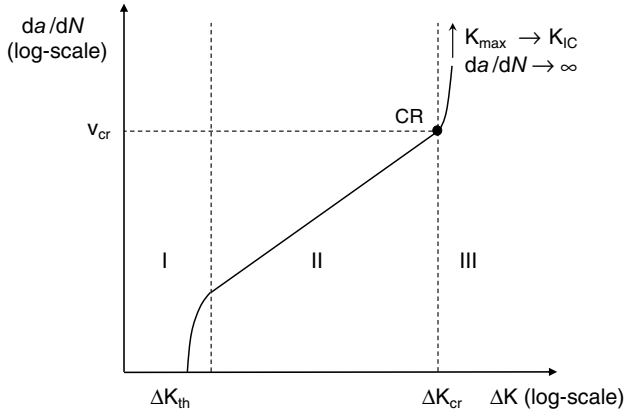

Fig. 1. Scheme of the typical fatigue crack propagation curve.

In Region II the Paris' equation [5,6] provides a good approximation to the majority of experimental data:

$$\frac{da}{dN} = C(\Delta K)^m, \tag{1}$$

where C and m are empirical constants usually referred to as Paris' law parameters.

From the early 1960s, research studies have been focused on the nature of the Paris' law parameters, demonstrating that C and m cannot be considered as material constants. In fact, they depend on the testing conditions, such as the loading ratio $R = \sigma_{min}/\sigma_{max} = K_{min}/K_{max}$ [7], on the geometry and size of the specimens [8–10] and, as pointed out very recently, on the initial crack length [11]. However, an important question regarding the Paris' law parameters still remains to be answered: are C and m independent of each other or is it possible to find a correlation between them based on theoretical considerations? Concerning this point, it is important to take note of the controversy in the literature about the existence of a correlation between C and m. For instance, Cortie [12] stated that the correlation is formal with a little physical relevance, and the high coefficient of correlation between C and m is due to the logarithmic data representation. Similar arguments were proposed in [13], where a correlation-free representation was presented. On the other hand, a very consistent empirical relationship between the Paris' law parameters was found by several authors [14,15] and supported by experimental results [3,14,16].

In this paper, the correlation existing between the Paris' law parameters is derived on the basis of theoretical arguments. To this aim, both self-similarity concepts [9] and the condition that the Paris' law instability corresponds to the Griffith–Irwin instability at the onset of rapid crack growth are profitably used. Comparing the functional expressions derived according to these two independent approaches, a relation between the Paris' law parameters C and m is proposed. As a result, it is shown that only one macroscopic parameter is needed for the characterization of damage during fatigue crack growth.

An experimental assessment of this new correlation is proposed for a wide range of materials including steels, titanium and aluminium alloys, as well as epoxy resins with liquid-filled urea–formaldehyde microcapsules and polymer/silica interfaces. The effect of the loading ratio on the parameter C is also analyzed.

2. Correlation derived according to self-similarity concepts

According to dimensional analysis, the physical phenomenon under observation can be regarded as a *black box* connecting the external variables (called input or governing parameters) with the mechanical response (output parameters). In case of fatigue crack growth in Region II, we assume that the mechanical response of the system is fully represented by the crack growth rate, $q_0 = da/dN$, which is the parameter to be determined. This output parameter is a function of a number of variables:

$$q_0 = F(q_1, q_2, \ldots, q_n; s_1, s_2, \ldots, s_m; r_1, r_2, \ldots, r_k), \tag{2}$$

where q_i are quantities with independent physical dimensions, i.e. none of these quantities has a dimension that can be represented in terms of a product of powers of the dimensions of the remaining quantities. Parameters s_i are such that their dimensions can be expressed as products of powers of the dimensions of the parameters q_i. Finally, parameters r_i are nondimensional quantities. According to the Buckingham's Π Theorem [17], the number of parameters involved in the problem can be reduced by n. According to this method, let us consider the n dimensionally independent quantities q_i $(i = 1,\ldots,n)$, so that the product $q_1^{\alpha_{10}} q_2^{\alpha_{20}} \cdots q_n^{\alpha_{n0}} = \prod_{i=1}^{n} q_i^{\alpha_{i0}}$ has the same dimensions as q_0 for a suitable choice of the values α_{i0}. Analogously, the product $q_1^{\alpha_{11}} q_2^{\alpha_{21}} \cdots q_n^{\alpha_{n1}} = \prod_{i=1}^{n} q_i^{\alpha_{i1}}$ can have the same dimensions as s_1 for suitable values of α_{i1}, and so on. As a result, the function (2) can be transformed as:

$$\frac{q_0}{q_1^{\alpha_{10}} q_2^{\alpha_{20}} \ldots q_n^{\alpha_{n0}}} = \Phi\left(\frac{s_1}{q_1^{\alpha_{11}} q_2^{\alpha_{21}} \ldots q_n^{\alpha_{n1}}}, \frac{s_2}{q_1^{\alpha_{12}} q_2^{\alpha_{22}} \ldots q_n^{\alpha_{n2}}}, \ldots, \frac{s_m}{q_1^{\alpha_{1m}} q_2^{\alpha_{2m}} \ldots q_n^{\alpha_{nm}}}; r_1, r_2, \ldots, r_k\right). \tag{3}$$

More synthetically, Eq. (3) can be written as:

$$\Pi_0 = \Phi(\Pi_1, \Pi_2, \ldots, \Pi_m; r_1, r_2, \ldots, r_k), \tag{4}$$

where the following nondimensional parameters have been introduced:

$$\Pi_0 = \frac{q_0}{q_1^{\alpha_{10}} q_2^{\alpha_{20}} \ldots q_n^{\alpha_{n0}}},$$
$$\Pi_j = \frac{s_j}{q_1^{\alpha_{1j}} q_2^{\alpha_{2j}} \ldots q_n^{\alpha_{nj}}}.$$

Relevant applications of this method in Solid Mechanics have concerned the analysis of complete and incomplete self-similarity of strength and toughness in disordered materials [18–23], as well as the study of the incomplete self-similarity in the linear range of fatigue crack growth, with special emphasis to size-scale effects [8,24].

As regards the phenomenon of fatigue crack growth, it is possible to consider the following functional dependence:

$$\frac{\mathrm{d}a}{\mathrm{d}N} = F(\sigma_y, K_{IC}, \omega; \Delta K, D, h, a_0; 1 - R), \tag{5}$$

where the governing variables are summarized in Table 1, along with their physical dimensions expressed in the Length–Force–Time class (LFT).

From this list it is possible to distinguish between three main categories of parameters. The first category regards the material parameters, such as the yield stress, σ_y, and the fracture toughness, K_{IC}. The second category comprises the variables governing the testing conditions, such as the stress–intensity factor range, ΔK, the loading ratio, R, and the frequency of the loading cycle, ω. Concerning environmental conditions and chemical phenomena, they are not considered as primary variables in this formulation and their influence on fatigue crack growth can be taken into account as a degradation of the material properties. Finally, the last category includes geometric parameters related to the material microstructure, such as the internal

Table 1
Governing variables of the fatigue crack growth phenomenon

Variable	Definition	Symbol	Dimensions
q_1	Tensile yield stress of the material	σ_y	FL^{-2}
q_2	Material fracture toughness	K_{IC}	$FL^{-3/2}$
q_3	Frequency of the loading cycle	ω	T^{-1}
s_1	Stress–intensity range	$\Delta K = K_{max} - K_{min}$	$FL^{-3/2}$
s_2	Characteristic structural size	D	L
s_3	Internal characteristic length	h	L
s_4	Initial crack length	a_0	L
r_1	Loading ratio	$R = \frac{K_{min}}{K_{max}}$	–

characteristic length, h, and to the tested geometry, such as the characteristic structural size, D, and the initial crack length, a_0.

Considering a state with no explicit time dependence, Eq. (3) becomes:

$$\frac{\mathrm{d}a}{\mathrm{d}N} = \left(\frac{K_{\mathrm{IC}}}{\sigma_{\mathrm{y}}}\right)^2 \Phi\left(\frac{\Delta K}{K_{\mathrm{IC}}}, \frac{\sigma_{\mathrm{y}}^2}{K_{\mathrm{IC}}^2} D, \frac{\sigma_{\mathrm{y}}^2}{K_{\mathrm{IC}}^2} h, \frac{\sigma_{\mathrm{y}}^2}{K_{\mathrm{IC}}^2} a_0; 1 - R\right), \tag{6}$$

where the nondimensional parameters are:

$$\begin{aligned}
\Pi_1 &= \tfrac{\Delta K}{K_{\mathrm{IC}}}, \\
\Pi_2 &= \tfrac{\sigma_{\mathrm{y}}^2}{K_{\mathrm{IC}}^2} D, \\
\Pi_3 &= \tfrac{\sigma_{\mathrm{y}}^2}{K_{\mathrm{IC}}^2} h, \\
\Pi_4 &= \tfrac{\sigma_{\mathrm{y}}^2}{K_{\mathrm{IC}}^2} a_0, \\
\Pi_5 &= r_1 = 1 - R.
\end{aligned}$$

It has to be noticed that Π_2 takes into account the effect of the specimen size and it corresponds to the square of the nondimensional number Z defined in [8], and to the inverse of the square of the *brittleness number s* introduced in [18,19,25]. Moreover, the parameter Π_4 is responsible for the dependence of the fatigue phenomenon on the initial crack length, as recently pointed out in [11].

At this point, we want to see if the number of the quantities involved in the relationship (6) can be reduced further from five. For example, starting from ΔK, this parameter can be considered as non-essential when, for very large or very small values of the corresponding nondimensional parameter Π_1, a finite non-zero limit of the function Φ exists:

$$\lim_{\Pi_1 \to 0 \text{ or } \Pi_1 \to \infty} \Phi(\Pi_1, \Pi_2, \Pi_3, \Pi_4, \Pi_5) = \Phi_1(\Pi_2, \Pi_3, \Pi_4, \Pi_5). \tag{7}$$

In this case we speak about *complete self-similarity*, or *self-similarity of the first kind* [9], in the parameter Π_1. On the other hand, if the limit of the function Φ tends to zero or infinity, the quantity Π_1 remains essential no matter how small or large it becomes. However, in some cases, the limit of the function Φ tends to zero or infinity, but the function Φ has a power-type asymptotic representation:

$$\lim_{\Pi_1 \to 0 \text{ or } \Pi_1 \to \infty} \Phi(\Pi_1, \Pi_2, \Pi_3, \Pi_4, \Pi_5) = \Pi_1^{\beta_1} \Phi_1(\Pi_2, \Pi_3, \Pi_4, \Pi_5), \tag{8}$$

where the exponent β_1 and, consequently, the nondimensional parameter Φ_1, cannot be determined from considerations of dimensional analysis alone. Moreover, the exponent β_1 may depend on the nondimensional parameters Π_i. In such cases, we speak about *incomplete similarity*, or *self-similarity of the second kind* [9], in the parameter Π_1. It is remarkable to notice that the parameter β_1 can only be obtained either from a best-fitting procedure on experimental results, or according to numerical simulations.

As regards the parameter ΔK, the corresponding nondimensional parameter Π_1 is usually small in the Region II of fatigue crack growth. However, since it is well-known that the fatigue crack growth phenomenon is strongly dependent on this variable (see e.g. the Paris' law in Eq. (1)), a complete self-similarity in Π_1 cannot be accepted. Hence, assuming an incomplete self-similarity in Π_1, we have:

$$\frac{\mathrm{d}a}{\mathrm{d}N} = \left(\frac{K_{\mathrm{IC}}}{\sigma_{\mathrm{y}}}\right)^2 \left(\frac{\Delta K}{K_{\mathrm{IC}}}\right)^{\beta_1} \Phi_1(\Pi_2, \Pi_3, \Pi_4, \Pi_5) = (K_{\mathrm{IC}}^{2-\beta_1} \sigma_{\mathrm{y}}^{-2}) \Delta K^{\beta_1} \Phi_1(\Pi_2, \Pi_3, \Pi_4, \Pi_5). \tag{9}$$

Repeating this reasoning for the parameter $(1 - R)$, which is a small number comprised between zero and unity, a complete self-similarity in Π_5 would imply that fatigue crack growth is independent of the loading ratio. However, this behavior is in contrast with some experimental results indicating an increase in the response $\mathrm{d}a/\mathrm{d}N$ when increasing the parameter R [26]. Therefore, assuming again an incomplete self-similarity in Π_5, we have:

$$\frac{da}{dN} = (K_{IC}^{2-\beta_1}\sigma_y^{-2})(1-R)^{\beta_2}\Delta K^{\beta_1}\Phi_2(\Pi_2,\Pi_3,\Pi_4). \tag{10}$$

Comparing Eq. (10) with the expression of the Paris' law, we find that our proposed formulation encompasses Eq. (1) as a limit case when:

$$m = \beta_1, \tag{11a}$$

$$C = (K_{IC}^{2-\beta_1}\sigma_y^{-2})(1-R)^{\beta_2}\Phi_2(\Pi_2,\Pi_3,\Pi_4) = (K_{IC}^{2-m}\sigma_y^{-2})(1-R)^{\beta_2}\Phi_2(\Pi_2,\Pi_3,\Pi_4). \tag{11b}$$

As a consequence, from Eq. (11b) it is possible to notice that the parameter C is dependent on two material parameters, such as the fracture toughness, K_{IC}, and the yield stress, σ_y, as well as on the loading ratio, R, and on the nondimensional parameters Π_2, Π_3 and Π_4. Moreover, Eq. (11b) demonstrates the existence of a relationship between the Paris' law parameters C and m. It is worth emphasizing that this result has been established according to dimensional analysis concepts and incomplete self-similarity assumptions in Π_1 and Π_5, which is a condition usually verified by experimental tests.

3. Correlation derived according to the crack growth instability condition

In this section we derive a correlation between the Paris' law parameters similar to that in Eq. (11b) on the basis of the condition of crack growth instability. In fact, as firstly pointed out by Forman et al. [4], the crack propagation rate, da/dN, is not only a function of the stress–intensity factor range, ΔK, but also on the condition of instability of the crack growth when the maximum stress–intensity factor approaches its critical value for the material.

Focusing our attention on this dependence, Forman et al. [4] observed that the crack propagation rate must tend to infinity when $K_{max} \to K_{IC}$, i.e.

$$\lim_{K_{max}\to K_{IC}} \frac{da}{dN} = \infty. \tag{12}$$

This rapid increase in the crack propagation rate is then responsible for the fast deviation from the linear part of the Region II in the fatigue plot (see e.g. Fig. 1). Considering the transition point-labelled CR in Fig. 1 between Region II and Region III, the following relationship between the crack growth rate and the stress–intensity factor range can be established according to the Paris' law:

$$\left(\frac{da}{dN}\right)_{CR} = v_{CR} = C(\Delta K_{CR})^m, \tag{13}$$

where ΔK_{CR} and v_{CR} denote the values of the coordinates of the point CR in Fig. 1. Due to the fact that a rapid variation in the crack propagation rate takes place when the onset of crack instability is reached, it is a reasonable assumption to consider the maximum stress–intensity factor evaluated at the point CR, K_{max}^{CR}, approximately equal to K_{IC}. As a consequence of this approximation, it is possible to correlate the value of ΔK_{CR} with the material fracture toughness:

$$\Delta K_{CR} \cong (1-R)K_{IC}. \tag{14}$$

Hence, introducing Eq. (14) into Eq. (13), an approximate relationship between the Paris' constants is derived according to the condition that the onset of the Paris' instability corresponds to the Griffith–Irwin instability:

$$v_{CR} \cong C[(1-R)K_{IC}]^m \quad \Rightarrow \quad C \cong v_{CR}\left[\frac{1}{(1-R)K_{IC}}\right]^m. \tag{15}$$

A closer comparison between Eqs. (15) and (11b) permits to clarify the role played by v_{CR}. In fact, Eq. (15) corresponds to the correlation derived according to self-similarity concepts when:

$$m = \beta_1 = -\beta_2, \tag{16a}$$

$$v_{CR} = \left(\frac{K_{IC}}{\sigma_y}\right)^2 \Phi_2(\Pi_2, \Pi_3, \Pi_4), \tag{16b}$$

confirming the experimental observation reported in [3] that v_{CR} depends on the material properties, on the geometry of the tested specimen, and on the material microstructure. Therefore, considering the same testing conditions, this conventional crack growth rate is almost constant for each class of material. This unique property of the point CR of the Paris' curve has also been recently confirmed by Farahmand [27], who analyzed more than one hundred fatigue crack growth curves of aerospace alloys and showed that the crack growth rate evaluated at the onset of the Region III, i.e. in correspondence of $K_{max} \cong K_{IC}$, is constant for many metallic alloys. As a result, Eq. (15) establishes a one-to-one correspondence between the C and m values. The dependence on the loading ratio is also put into evidence in Eq. (15).

4. Extension to interface fatigue crack propagation

The fatigue life of bi-material interfaces can be characterized using either a stress-life approach, or using a defect-tolerant method [28]. In the former case, the number of loading cycles required to both initiate and grow a debond to a critical length is measured, whereas in the latter attention is devoted to characterize the debond growth rate behavior. According to this second approach, experimental data are usually represented in terms of the subcritical debond growth rate, $\mathrm{d}a/\mathrm{d}N$, where a is the debond length and N is the cycles number, as a function of the strain energy release rate range, $\Delta\mathscr{G} = \mathscr{G}_{max} - \mathscr{G}_{min}$.

From experiments it has been found that the intermediate debond growth rates can be modeled according to a Paris-like power-law relationship [29]:

$$\frac{\mathrm{d}a}{\mathrm{d}N} = C^*(\Delta\mathscr{G})^{m^*}, \tag{17}$$

where C^* and m^* are empirically derived fitting parameters. Usually, the exponent m^* ranges from 1 to 3 for metals, from 2 to 5 for bulk polymers, whereas for brittle ceramic materials m^* is larger than 6.

In this case the Griffith–Irwin instability corresponds to the Paris' instability when the maximum strain energy release rate approaches the critical value for the material, i.e. $\mathscr{G}_{max} \to \mathscr{G}_{IC}$. As a consequence, following the same reasoning as in Section 3, the following theoretically-based relationship between the parameters C^* and m^* in Eq. (17) can be obtained:

$$C^* = v_{CR}\left[\frac{1}{\Delta\mathscr{G}_{CR}}\right]^{m^*}. \tag{18}$$

Moreover, according to the well-known Irwin relationship relating the critical strain energy release rate with the fracture toughness, i.e. $\mathscr{G}_{IC} = K_{IC}^2/E$ for plane stress conditions, Eq. (18) can be rewritten in terms of K_{IC}:

$$C^* \cong v_{CR}\left[\frac{E}{(1-R)^2 K_{IC}^2}\right]^{m^*}. \tag{19}$$

Comparing Eqs. (19) and (15), we find out the relationship existing among the coefficients m^* and C^* and the coefficients m and C of the Paris' law in Eq. (1):

$$\begin{aligned} m^* &= m/2, \\ C^* &= C \cdot E^{m/2}. \end{aligned}$$

5. Experimental assessment of the proposed correlation

Parameters C and m entering the Paris' law are usually impossible to estimate according to theoretical considerations and fatigue tests have to be performed. However, many authors [3,14,30] experimentally observed

a very stable relationship between the parameters C and m, which is usually represented by the following empirical formula:

$$C = AB^m, \tag{20}$$

usually written in a logarithmic form:

$$\log C = \log A + m \log B. \tag{21}$$

Taking the logarithm of both sides of the theoretically-based relationship between C and m in Eq. (15), we obtain

$$\log C = \log v_{CR} + m \log \left[\frac{1}{(1-R)K_{IC}} \right] \tag{22}$$

which corresponds to Eq. (21) if

$$A = v_{CR}, \tag{23a}$$

$$B = \frac{1}{(1-R)K_{IC}}. \tag{23b}$$

In order to check the validity of the proposed correlation derived according to the instability condition of the crack growth, an experimental assessment is performed by comparing the experimentally determined values of B for steels, titanium and aluminium alloys, as well as for epoxy resins and polymer/silica interfaces, with those theoretically predicted according to Eq. (23b). The effect of the loading ratio is also discussed.

5.1. Aluminium, titanium and steel alloys

In this section the effectiveness of our proposed correlation between the Paris' law parameters derived according to the instability condition of the crack growth is checked in reference to aluminium, titanium and steel alloys. To this aim, we consider the experimental data reported in [27] and determined according to the NASGRO program [31], which is one of the most comprehensive database of fatigue crack growth curves for aerospace alloys. These experimental data concern the material fracture toughness, the Paris' law parameters, as well as the crack growth rate corresponding to $K_{max} \cong K_{IC}$ for fatigue tests with $R = 0$ (see Table 2). As previously outlined, the fracture toughness data and the values of v_{CR} are almost constant for each class of materials. This property is very well evidenced by the 2219-T62, 2219-T87, 6061-T62 and 7075-T73 aluminium alloys.

The application of Eq. (15) permits to predict the value of the Paris' law parameter C as a function of m and to compare it with the experimental one reported in the fifth column of Table 2. The agreement between the experimental data and the predictions made according to our correlation is noticeably good, as also evidenced by the relative percentage error reported in the last column of Table 2.

A sensitivity analysis of the parameter C to the variation in fracture toughness data can also be performed in reference to steels and aluminium alloys. For these materials, Radhakrishnan [14] collected a number of

Table 2
Experimental assessment of the proposed correlation for aluminium, titanium and steel alloys according to the NASGRO database [27]

Material	Experimental data				Present correlation	
	K_{IC} (MPa$\sqrt{m}$)	v_{CR} (m/cycle)	m	C	C	Relative error (%)
Alum-2219-T62 (L-T)	28.2	3.5×10^{-6}	2.87	2.40×10^{-10}	2.41×10^{-10}	0
Alum-2219-T87 (L-T)	27.3	3.5×10^{-6}	3.30	6.27×10^{-11}	6.38×10^{-11}	2
Alum-6061-T62 (L-T)	25.0	3.5×10^{-6}	3.20	1.63×10^{-10}	1.18×10^{-10}	−28
Alum-7075-T73, Forged (L-T)	27.3	3.5×10^{-6}	2.98	1.80×10^{-10}	1.84×10^{-10}	2
Pure titanium (Fty = 380 MPa)	46.0	1.0×10^{-5}	3.41	1.95×10^{-11}	2.14×10^{-11}	10
Ti–6Al–4V-RT (mill annealed)	15.5	2.0×10^{-7}	3.11	3.80×10^{-11}	3.97×10^{-11}	4
PH13-8Mo-H1000 (steel alloy)	100.0	3.0×10^{-5}	3.40	5.00×10^{-12}	4.75×10^{-12}	−5

data from various sources and proposed the following least square fitting relationships (ΔK being in ksi$\sqrt{\text{inch}}$ and da/dN in inch/cycle):

$$\begin{aligned} &\log C = \log(3\times 10^{-5}) + m\log(1.99\times 10^{-2}) \quad \text{for steels,} \\ &\log C = \log(1\times 10^{-4}) + m\log(4.68\times 10^{-2}) \quad \text{for Al alloys.} \end{aligned} \tag{24}$$

These relationships are also consistent with more recent studies proposed by Kitagawa [3] and with several correlations reported in fatigue handbooks (see e.g. [32]). In S.I. they read (ΔK being in MPa$\sqrt{\text{m}}$ and da/dN in m/cycle):

$$\log C = \log(7.6\times 10^{-7}) + m\log(1.81\times 10^{-2}) \quad \text{for steels,} \tag{25a}$$

$$\log C = \log(2.5\times 10^{-6}) + m\log(4.26\times 10^{-2}) \quad \text{for Al alloys.} \tag{25b}$$

As shown in Eq. (23a), the coefficient B can be theoretically predicted as a function of R and K_{IC}. To avoid experimental tests, which could be in general rather expensive and time consuming, the values of the material fracture toughness can be taken from selected handbooks. In this case, however, a certain dispersion in the collected data may exist, because the reported values are related to different testing conditions and specimen geometries.

Concerning steels, we assume $A = v_{CR} = 7.6\times 10^{-7}$ m/cycle, as experimentally determined by Radhakrishnan, $R = 0$, and we try to estimate the parameter B and its sensitivity to the variation of K_{IC} on the basis of the values of the fracture toughness reported in the ASM handbook [32]. This book provides a collection of values in a diagram K_{IC} vs. both the prior austenite grain size, and the temperature test. Over a large range of temperatures (T from -269 °C to 27 °C) and grain sizes (d from 1 μm to 16 μm), K_{IC} varies from 20 MPa$\sqrt{\text{m}}$ to 100 MPa$\sqrt{\text{m}}$ with an average value of $\overline{K}_{IC} = 60$ MPa$\sqrt{\text{m}}$. Using these data we find:

$$\log C \cong \log(7.6\times 10^{-7}) + m\log(1.67\times 10^{-2} + \delta B), \tag{26}$$

where δB is related to the fracture toughness excursion from the average value, $\delta K_{IC} = 40$ MPa$\sqrt{\text{m}}$, as:

$$\delta B = \frac{\mp \delta K_{IC}}{(\overline{K}_{IC} \pm \delta K_{IC})\overline{K}_{IC}} = \begin{cases} +3.3\times 10^{-2} \\ -6.7\times 10^{-3} \end{cases} \tag{27}$$

A good agreement between the proposed estimation based on an average value of the critical stress–intensity factor and the experimental relationship in Eq. (25a) by Radhakrishnan [14] for steels is achieved, as clearly shown in Fig. 2a (see the dashed-dotted line compared with the solid line). The curves log C vs. log m obtained using the maximum and the minimum values of K_{IC} are also reported in Fig. 2a with dashed lines.

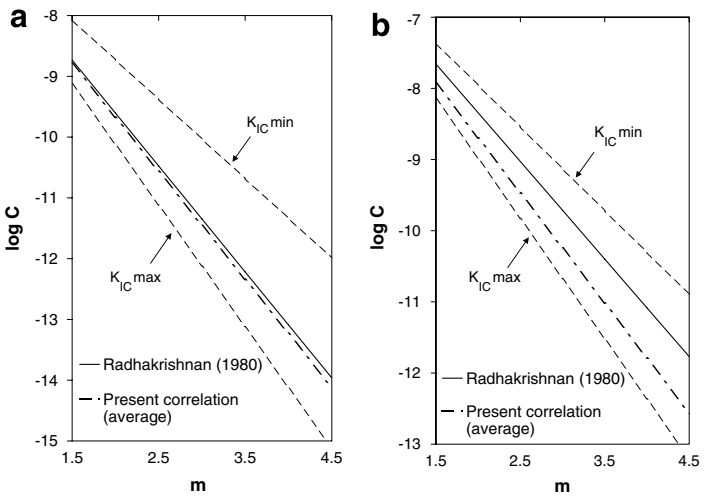

Fig. 2. Proposed correlation between Paris' law parameters C and m for (a) steels and (b) aluminium alloys.

The comparison can also be extended to aluminium alloys, assuming $A = v_{CR} = 2.5 \times 10^{-6}$ m/cycle from the Radhakrishnan correlation in Eq. (25b). According to the same procedure discussed above, the estimated average value of the critical stress–intensity factor from handbooks [32–35] is equal to $\overline{K}_{IC} = 35$ MPa$\sqrt{\text{m}}$ with minimum and maximum values equal to 15 MPa$\sqrt{\text{m}}$ and 49 MPa$\sqrt{\text{m}}$, respectively. According to these data we find:

$$\log C \cong \log(2.5 \times 10^{-6}) + m \log(2.86 \times 10^{-2} + \delta B), \tag{28}$$

where δB is equal to

$$\delta B = \frac{\mp \delta K_{IC}}{(\overline{K}_{IC} \pm \delta K_{IC})\overline{K}_{IC}} = \begin{cases} +3.8 \times 10^{-2} \\ -8.2 \times 10^{-3} \end{cases} \tag{29}$$

Also in this case, a good agreement between the proposed estimation based on an average value of the critical stress–intensity factor and the experimental relationship in Eq. (25b) for Al alloys is achieved (see Fig. 2b).

5.2. Epoxy resins

The proposed correlation based on the instability condition provides also a good estimation of C for epoxy resins. Brown et al. [36,37] experimentally computed Paris' law parameters and the critical stress–intensity factor for brittle and fatigue crack propagation in an epoxy matrix with liquid-filled urea–formaldehyde microcapsules. Interestingly, with a microcapsule concentration higher than 10 wt%, fracture parameters are almost constant and are reported in Table 3. In this case, the average fracture toughness is equal to $\overline{K}_{IC} = 1.1$ MPa$\sqrt{\text{m}}$, whereas average Paris' law parameters are $\bar{m} = 4.55$ and $\overline{C} = 9.4 \times 10^{-7}$, respectively. Observing from the experiments in [36] that the crack growth rate at the onset of crack instability, v_{CR}, is equal to 4×10^{-7} m/cycle and that $R = 0.1$, we have:

$$C \cong v_{CR}\left[\frac{1}{(1-R)\overline{K}_{IC}}\right]^{\bar{m}} = 4.2 \times 10^{-7}, \tag{30}$$

in a rather good agreement with the average value of C experimentally determined from fatigue tests.

5.3. Polymer/silica interfaces

The applicability of the proposed correlation to interface fracture problems can be assessed using the experimental data by Snodgrass et al. [29]. They experimentally studied the phenomenon of subcritical debonding of polymer/silica interfaces under both monotonic and cyclic loading with and without an adhesion promoter. For an interface without adhesion promoters, they found the following parameters, considering $R = 0.1$:

$$\mathscr{G}_{IC} = 10.1 \text{ J/m}^2,$$
$$m^* = 6.0,$$
$$C^*_{exp} = 4.0 \times 10^{-13}.$$

Table 3
Fatigue parameters of microcapsule toughened epoxy [36]

Microcapsule concentration (wt%)	Diameter (μm)	K_{IC} (MPa$\sqrt{\text{m}}$)	C	m
10	50 ± 20	1.20	1.5×10^{-3}	4.9
20	50 ± 20	1.10	1.6×10^{-3}	4.6
10	180 ± 40	1.20	5.4×10^{-4}	4.4
20	180 ± 40	1.00	3.8×10^{-4}	4.3
10	460 ± 80	0.92	7.8×10^{-4}	4.4
20	460 ± 80	1.20	8.6×10^{-4}	4.7

Estimating $v_{CR} \cong 1 \times 10^{-7}$ m/cycle in correspondence of $\Delta\mathscr{G}_{CR} = (1-R)^2\mathscr{G}_{IC} = 8.2$ J/m^2 from the fatigue plot in [29], we theoretically predict the value of the Paris' law parameter C^* as a function of m^* according to Eq. (18):

$$C^*_{th} \cong v_{CR}\left[\frac{1}{(1-R)^2\mathscr{G}_{IC}}\right]^{m^*} = 3.3 \times 10^{-13}.$$

For an interface with Amino-silane AP8000 as an adhesion promoter, they found the following parameters ($R = 0.1$):

$$\mathscr{G}_{IC} = 18 \text{ J/m}^2,$$
$$m^* = 6.2,$$
$$C^*_{exp} = 4.2 \times 10^{-14}.$$

Using $v_{CR} \cong 6 \times 10^{-7}$ m/cycle in correspondence of $\Delta\mathscr{G}_{CR} = (1-R)^2\mathscr{G}_{IC} = 14.6$ J/m^2 from the fatigue plot in [29], we have:

$$C^*_{th} \cong v_{CR}\left[\frac{1}{(1-R)^2\mathscr{G}_{IC}}\right]^{m^*} = 3.65 \times 10^{-14}.$$

In both cases, the theoretically predicted values, C^*_{th}, are in fair good agreement with the experimentally computed ones, C^*_{exp}. This implies that it is possible to theoretically predict the Paris' law parameter C^* from the unique properties of the critical point CR. Moreover, as also pointed out in the previous examples, the obtained correlation can be generalized to other testing conditions, e.g. characterized by different loading ratios, since the coordinates of the point CR are almost constant for a given material (see also Section 5.1 and [27]).

5.4. Effect of the loading ratio

Experimental results on fatigue crack growth show that, in most cases, the crack growth rate is not only a function of the stress–intensity range, ΔK, but also of the mean stress level. This parameter is usually taken into account in fatigue analyses through either the stress ratio, $R = K_{min}/K_{max}$, or, equivalently, using the maximum stress–intensity factor, K_{max}. Hence, several authors proposed improved expressions of the Paris' law, explicitly considering the effect of R or K_{max} in the formulations:

$$\frac{da}{dN} = f(\Delta K, R) = g(\Delta K, K_{max}). \tag{31}$$

For instance, for different types of materials, Roberts and Erdogan [38], Klesnil and Lukas [39], Hojo et al. [40], Liu and Chen [41] and Walker [42] proposed similar equations including both R and ΔK:

$$\frac{da}{dN} = C'(1-R)^p(\Delta K)^{m'}. \tag{32}$$

The effect of the crack closure was also modeled in this framework by Kujawski [43]. Since the exponent p is negative, Eq. (32) implies that the crack propagation rate in Region II is larger for higher R ratios. Although these formulations are consistent with the results obtained according to self-similarity concepts and can be recovered by putting $\beta_1 = m'$ and $\beta_2 = p$ in Eq. (10), they introduce another independent parameter, say p, to describe the phenomenon of fatigue crack growth.

On the other hand, empirical formulae where the exponent of the term dependent on R is the same as that for the stress–intensity factor range are also available in the literature, as reported in [3]:

$$\frac{da}{dN} = C(A + BR)^m(\Delta K)^m, \tag{33}$$

where A, B and C are determined from experiments. Moreover, it has to be noticed that, for some materials such as 4.5% Cu–Al Alloy, 5% Mg–Al Alloy, 5.5% Zn–Al Alloy, HS 30 W Al Alloy, 7075-T6 Al Alloy and HT 80 Steel, Radhakrishnan [7] found that the parameter C is almost independent of the loading ratio, whereas a

dependence on R was observed for the exponent m. Also this behavior can be interpreted in the framework of the correlation based on incomplete self-similarity by considering $\beta_2 = 0$ and $\beta_1 = \beta_1(\Pi_5)$ in Eq. (10).

Considering the approximate relationship derived according to the condition of crack growth instability, Eq. (15), the exponent of the term $(1 - R)$ is strictly related to that of ΔK, that is $\beta_1 = m$ and $\beta_2 = -m$. An experimental assessment of this formulation can be proposed by considering the experimental data provided by Lee and Lee [16]. They performed fatigue tests on 2024-T4 and 2024-T6 aluminium alloys under different values of the loading ratio and computed the parameters A and B in Eq. (21). In particular, for $R = 0$ they found $\log A = -6.74$ and $\log B = -1.04$, whereas for $R = 0.3$ they obtained $\log A = -7.09$ and $\log B = -0.85$.

As regards the correlation between C and m derived according to the condition of crack growth instability, the logarithm of the parameter A should be independent of R, since it corresponds to the critical crack growth rate, v_{CR}, which is a conventional crack growth rate approximately constant for each class of materials. On the other hand, the logarithm of the parameter B should depend on R according to Eq. (23b). Observing, that $\log K_{IC} = -\log B$ for $R = 0$ (see Eqs. (21) and (22)), the relative variations of the parameters $\log A$ and $\log B$ due to a change in the loading ratio from 0.0 to 0.3 can be theoretically predicted as:

$$\delta(\log A) = 0\%,$$
$$\delta(\log B) = \frac{\log B_{R=0.3} - \log B_{R=0}}{\log B_{R=0}} = \frac{\log(1-R)}{\log K_{IC}} = 15\%.$$

These results are consistent with the variation of the parameters A and B computed from the experimental data in [16]:

$$\delta(\log A) = \frac{-7.09+6.74}{-6.74} = 5\%,$$
$$\delta(\log B) = \frac{-0.85+1.04}{-1.04} = 18\%.$$

6. Discussion and conclusion

To shed light on the controversy about the existence of a correlation between the Paris' constants, both self-similarity concepts and the condition that the Paris' law instability corresponds to the Griffith–Irwin instability at the onset of rapid crack growth have been profitably used. Comparing the functional expressions derived from these two independent approaches, an approximate relationship between C and m has been proposed. According to this theory, it is found that the parameter C is also dependent on the fracture toughness of the material, on the crack growth rate at the onset of crack instability, and on the loading ratio. The main consequence of this correlation is that only one macroscopic parameter is needed for the characterization of damage during fatigue crack growth. A good agreement between the theoretical predictions obtained using this correlations and extensive experimental data has been achieved. In this respect, a special emphasis has been given to the effect of the loading ratio.

From the engineering standpoint, it has to be emphasized that our proposed correlation constitutes a useful tool for design purposes. In fact, in case of a lack of experimental fatigue data for a new material to characterize, one could, as a first approximation, determine the parameter C as a function of the exponent m according to Eq. (15). Then, a parametric analysis by varying the exponent m in its usual range of variation can be performed and numerical simulations of fatigue crack growth can be put forward. Parameters v_{CR} and K_{IC} entering the correlation can be either known in advance, or estimated from materials with similar composition, thermal treatment and mechanical properties (see e.g. [44,45]).

A final remark concerns the fundamental question posed by Forman et al. [4]: "does material embrittlement due to strain cycling or temperature effects cause changes in all three material constants, K_{IC}, C, m, or in only the fracture toughness?". Since a dependence of the parameter C on the fracture toughness has been put into evidence in our proposed correlation, it is expected that not only the fracture toughness is affected by material embrittlement, but, consequently, also the fatigue parameter C.

Acknowledgement

Support of the Italian Ministry of University and Research (MIUR) is gratefully acknowledged.

References

[1] Ritchie RO. Influence of microstructure on near-threshold fatigue-crack propagation in ultra-high strength steel. Met Sci 1977;11:368–81.
[2] Taylor D. Fatigue thresholds. London: Butterworth; 1981.
[3] Kitagawa H. Introduction to fracture mechanics of fatigue. In: Carpinteri An, editor. Handbook of fatigue crack propagation in metallic structures, vol. I. Elsevier Science B.V.; 1994. p. 47–105.
[4] Forman RG, Kearney VE, Engle RM. Numerical analysis of crack propagation in cyclic-loaded structures. ASME J Basic Engng 1967;89:459–64.
[5] Paris PC, Gomez MP, Anderson WP. A rational analytic theory of fatigue. Trend Engng 1961;13:9–14.
[6] Paris PC, Erdogan F. A critical analysis of crack propagation laws. ASME J Basic Engng 1963;85D:528–34.
[7] Radhakrishnan VM. Parameter representation of fatigue crack growth. Engng Fract Mech 1979;11:359–72.
[8] Barenblatt GI, Botvina LR. Incomplete self-similarity of fatigue in the linear range of fatigue crack growth. Fatigue Fract Engng Mater Struct 1980;3:193–202.
[9] Barenblatt GI. Scaling, self-similarity and intermediate asymptotics. Cambridge: Cambridge University Press; 1996.
[10] Barenblatt GI. Scaling phenomena in fatigue and fracture. Int J Fract 2006;138:19–35.
[11] Spagnoli A. Self-similarity and fractals in the Paris range of fatigue crack growth. Mech Mater 2005;37:519–29.
[12] Cortie MB. The irrepressible relationship between the Paris law parameters. Engng Fract Mech 1988;30:49–58.
[13] Bergner F, Zouhar G. A new approach to the correlation between the coefficient and the exponent in the power law equation of fatigue crack growth. Int J Fatigue 2000;22:229–39.
[14] Radhakrishnan VM. Quantifying the parameters in fatigue crack propagation. Engng Fract Mech 1980;13:129–41.
[15] Tóth L, Krasowsky A Ja. Fracture as the result of self-organised damage process. J Mater Process Technol 1995;53:441–51.
[16] Lee JB, Lee DN. Correlation of two constants in the Paris equation for fatigue crack propagation rate in region II. Proceedings of the 6th international conference on fracture ICF6, New Delhi, India. Pergamon Press; 1984. p. 1727–33.
[17] Buckingham E. Model experiments and the form of empirical equations. ASME Trans 1915;37:263–96.
[18] Carpinteri A. Notch sensitivity in fracture testing of aggregative materials. Engng Fract Mech 1982;16:467–81.
[19] Carpinteri A. Plastic flow collapse vs. separation collapse in elastic–plastic strain-hardening structures. RILEM Mater Struct 1983;16:85–96.
[20] Carpinteri A. Size effects on strength, toughness and ductility. J Engng Mech 1989;115:1375–92.
[21] Carpinteri A. Cusp catastrophe interpretation of fracture instability. J Mech Phys Solids 1989;37:567–82.
[22] Carpinteri A. Scaling laws and renormalization groups for strength and toughness of disordered materials. Int J Solids Struct 1994;31:291–302.
[23] Carpinteri A. Strength and toughness in disordered materials: complete and incomplete similarity. In: Size-scale effects in the failure mechanisms of materials and structures, proceedings of the international union of theoretical and applied mechanics (IUTAM), Turin, Italy, London. E & FN Spon; 1994. p. 3–26.
[24] Ritchie RO. Incomplete self-similarity and fatigue-crack growth. Int J Fract 2005;132:197–203.
[25] Carpinteri A. Static and energetic fracture parameters for rocks and concretes. Mater Struct 1981;14:151–62.
[26] in Milne I, Ritchie RO, Karihaloo B, editors. Comprehensive structural integrity: fracture of materials from nano to macro. Cyclic loading and fatigue, vol. 4. Amsterdam: Elsevier; 2003.
[27] Farahmand B. Analytical method of generating da/dN curves for aerospace alloys. In: Gdoutos EE, editor. Fracture of nano and engineering materials and structures (Proceedings of the 16th European conference of fracture, Alexandroupolis, Greece, 2006), Paper No. 140 on CD–ROM, Dordrecht, 2006. Springer.
[28] M. Paggi. Interface mechanical problems in heterogeneous materials. PhD thesis, Politecnico di Torino, 2005.
[29] Snodgrass JM, Pantelidis D, Jenkins ML, Bravman JC, Dauskardt RH. Subcritical debonding of polymer/silica interfaces under monotonic and cyclic loading. Acta Mater 2002;50:2395–411.
[30] Niccolls EH. A correlation for fatigue crack growth rate. Scripta Metall 1976;10:295–8.
[31] Forman RG, Shivakumar V, Newman JC. Fatigue crack growth computer program NASA/FLAGRO. Technical Report JSC-22267A, NASA, January; 1993.
[32] ASM International. Fatigue and fracture resistance of ferrous alloys in ASM Handbook, vol.19. Ohio, Materials Park; 1987.
[33] Boyer HE, Gall TL, editors. Metals handbook. Materials Park, Ohio: American Society for Metals; 1985.
[34] Metals handbook, vol. 2 – Properties and selection: nonferrous alloys and special – purpose materials. 10th ed. ASM International; 1990.
[35] Ho CY, editor. Structural alloys handbook. CINDAS/Purdue University, West Lafayette, IN; 1996.
[36] Brown EN, White SR, Sottos NR. Fatigue crack propagation in microcapsule toughened epoxy; submitted for publication.
[37] Brown EN, White SR, Sottos NR. Retardation and repair of fatigue cracks in a microcapsule toughened epoxy composite—part I: manual infiltration. Compos Sci Technol 2005;65:2466–73.
[38] Roberts R, Erdogan F. The effect of mean stress on fatigue crack propagation in plates under extension and bending. ASME J Basic Engng 1967;89:885–92.
[39] Klesnil M, Lukas P. Effect of stress cycle asymmetry on fatigue crack growth. Mater Sci Engng 1972;9:231–40.
[40] Hojo M, Tanaka K, Gustafson CG, Hayashi R. Effect of stress ratio on near-threshold propagation of delamination fatigue cracks in unidirectional CFRP. Comput Sci Technol 1987;29:273–92.

[41] Liu S-Y, Chen I-W. Fatigue of yttria-stabilized zirconia. I: fatigue damage, fracture damage, fracture origins, and lifetime prediction. J Am Ceram Soc 1991;74:1197–205.
[42] Walke K. The effect of stress ratio during crack propagation and fatigue for 2024-T3 and 7075-T6 Aluminium. In: Effects of environments and complex and complex load history on fatigue life. ASTM STP 462. Philadelphia, PA; 1970. p. 1–14.
[43] Kujawski D. A fatigue crack driving force parameter with load ratio effects. Int J Fatigue 2001;23:S239–46.
[44] Pugno N, Ciavarella M, Cornetti P, Carpinteri A. A generalized Paris' law for fatigue crack growth. J Mech Phys Solids 2006;54:1333–49.
[45] Pugno N, Cornetti P, Carpinteri A. New unified laws in fatigue: from the Wöhler to the Paris' regime. Engng Fract Mech 2007;74:595–601.